

# Chapter 45

## Improved SQUID Sensors for Biomagnetic Imaging

Antonio Vettoliere, C. Granata, S. Rombetto and M. Russo

**Abstract** Improved niobium-based SQUID sensors in a magnetometer and a gradiometer configuration are presented. The SQUID magnetometer has an integrated square superconducting sensing coil with an area of  $9 \text{ mm}^2$ , much smaller than a typical SQUID magnetometers keeping a comparable magnetic field sensitivity but a higher spatial resolution. At  $T = 4.2 \text{ K}$ , an intrinsic magnetic field noise spectral density of  $5.8 \text{ fT}/\sqrt{\text{Hz}}$ , has been measured in the flux locked loop configuration. The SQUID planar gradiometer with a long baseline ( $50 \text{ mm}$ ) has a pickup antenna consisting of a series of two integrated rectangular coils inductively coupled to the SQUID in a double washer configuration. At  $T = 4.2 \text{ K}$  a magnetic flux noise spectral density of  $3 \mu\Phi_0/\sqrt{\text{Hz}}$  has been measured. The spectral density of the magnetic field noise referred to one sensing coil, is  $3.0 \text{ fT}/\sqrt{\text{Hz}}$  resulting in a gradient spectral noise of  $0.6 \text{ fT}/\text{cm} \cdot \sqrt{\text{Hz}}$ .

### 45.1 Miniaturized SQUID Magnetometer

Magnetometers based on the superconducting quantum interference device (SQUID) are very sensitive low-frequency magnetic field sensors and are widely used in several applications which require a high magnetic field sensitivity [1]. One of the most interest is in biomagnetic imaging. Since the magnetic flux noise increase with the SQUID inductance, to increase sensitivity an integrated superconducting flux transformer is used. To ensure the necessary magnetic field

---

A. Vettoliere (✉) · C. Granata · S. Rombetto · M. Russo  
Istituto di Cibernetica “E. Caianiello” del CNR,  
via Campi Flegrei, 34 - 80078, Pozzuoli (NA), Italy  
e-mail: a.vettoliere@cib.na.cnr.it

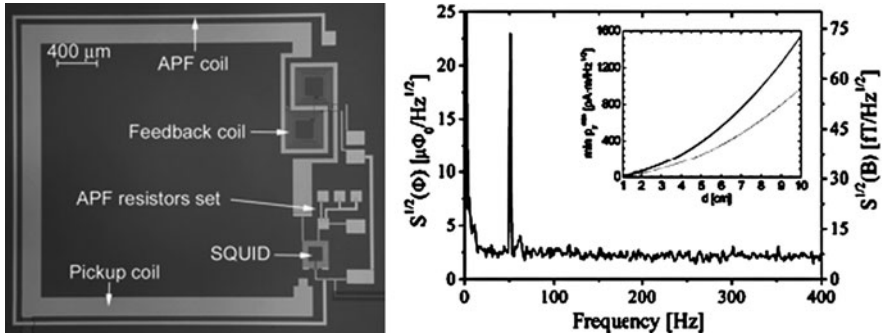


**Fig. 45.1** Picture of a fully integrated SQUID magnetometer (*left figure*). Magnetic flux noise spectral density, measured, at  $T = 4.2$  K, in FLL configuration (*right figure*). The inset shows the minimum dipole detectable by the sensors as a function of the relative distance

sensitivity for biomagnetic applications the devices have typically an area no less than  $60 \text{ mm}^2$  [1], limiting the number of sensors that can be allocated in biomagnetic systems.

Here, a high sensitive miniaturized dc SQUID magnetometer based on niobium technology is reported. It is a fully integrated device having an area less than  $10 \text{ mm}^2$  which includes a superconducting flux transformer consisting of a square pickup coil with a side length and width of 3 mm and 0.2 mm respectively; in series with a 8-turn input coil, which is coupled to the SQUID loop in a washer configuration; it also includes an additional positive feedback (APF) circuit and a bipolar feedback coil for low cross-talk operations. Apart from a better spatial resolution, a small pick-up coil minimizes its antenna gain reducing the effects of radio frequency interference. In order to improve the coupling properties between the SQUID and the input circuitry, a SQUID with a large inductance (250 pH) has been used. The consequent sensitivity degradation, due to non-optimal noise conditions, has been avoided by inserting of a damping resistor across the SQUID loop [2]. Such design allows to obtain a suitable flux-to-field conversion efficiency ( $B_\Phi$ ) and a high flux gain  $G_\Phi$ , that is the ratio between the magnetic flux threading the SQUID loop ( $\Phi_S$ ) and that one applied to the pick-up coil ( $\Phi_p$ ). The integrated APF circuit reduces the equivalent preamplifier flux noise with respect to the SQUID one in the case of direct-coupling readout scheme. It makes the voltage to magnetic flux characteristic ( $V-\Phi$ ) asymmetric, so, if the SQUID is biased on the steeper side, an effective increase of the SQUID responsivity ( $V_\Phi = \partial V / \partial \Phi$ ) is achieved [3]. The bipolar design of the feedback coil consisting of two multiturn coil allows to reduce cross-talk between neighboring sensors [4]. The sample fabrication process, capable to routinely produce high quality window-type junctions, has been well described elsewhere [4]. A picture of the device is shown in Fig. 45.1. The SQUID sensors have been characterized at  $T = 4.2$  K in a high shielded environment. A  $B_\Phi = 3.2 \text{ nT}/\Phi_0$  has been measured by applying an external magnetic field by means of calibrated Helmholtz coils. By using a low noise read-out electronics based on Flux Locked Loop (FLL) with a direct

coupling scheme, an intrinsic flux noise spectral density as low as  $2.2 \mu\Phi_0/\sqrt{\text{Hz}}$  in the white region, corresponding to  $7.0 \text{ fT}/\sqrt{\text{Hz}}$ , has been measured (Fig. 45.1). The intrinsic noise obtained by subtracting the amplifier contribution is  $5.8 \text{ fT}/\sqrt{\text{Hz}}$  [5]. The minimum value of current dipole detectable by this magnetometer and a typical one, having a 9 mm pickup coil side length and a suitable sensitivity for biomagnetic applications, have been computed and compared showing that the differences are appreciable only for deeper source (inset of Fig. 45.1) [6].

## 45.2 Planar SQUID Gradiometer

Since background noise signals exceed those of the biomagnetic sources by many orders of magnitude, both high shielded room and sophisticated noise cancellation techniques must be employed. In spite of this, hardware or electronic gradiometers are typically used to increase signal–noise ratio [7].

Here, a fully integrated first order planar SQUID gradiometer is presented. It has a high intrinsic balance thanks to the precision of the photolithographic techniques used in the fabrication process [8]. Moreover, the inductances of pickup and input coils are well matched ensuring a good signal coupling with the SQUID. Furthermore, the unreliable superconducting soldering are avoided. The pickup antenna consists of a series of two rectangular coils ( $12 \times 10 \text{ mm}^2$ ) having a distance between their center (baseline) of 50 mm, guaranteeing a suitable sensitivity also to the deep biomagnetic sources. The pickup coil, with a total inductance  $L_p = 90 \text{ nH}$ , is connected in series with an input coil consisting of a series of two coils (16 turns each), magnetically coupled to SQUID loop having a parallel double washer configuration. The inductances of the input coil and the SQUID are respectively  $L_i = 90 \text{ nH}$  and  $L_S = 109 \text{ pH}$  and the relative mutual inductance is  $M_i = 3.4 \text{ nH}$ . The device includes an integrated feedback coil for Flux Locked Loop operation (FLL), consisting of two multiturn coils (10 turns each) in a bipolar design allowing to reduce crosstalk between neighboring sensors [4]. The high intrinsic voltage-to-flux conversion factor  $V_\phi$  (responsivity), obtained increasing a critical current, reduces the flux noise contribution of the preamplifier to a tolerable value. To prevent a noise performance degradation, a thin film resistor across the SQUID inductance has been inserted [2]. It also eliminates possible washer resonances and guarantees smooth  $V-\Phi$  characteristics. The fabrication process is well described in Ref. [3]. In Fig. 45.2, a picture of the device and its particulars is shown. The read-out electronic for the measurements of both  $V-\Phi$  characteristics and noise performances is integrated on a very-low-noise miniaturized detection circuit having radio frequency filters on the electrical connections to room temperature. In such a configuration the SQUID is directly coupled to a preamplifier, which contributes to the overall magnetic flux noise by adding the term  $S_{V,\text{amp}}^{1/2}/V_\phi$  where  $S_{V,\text{amp}}^{1/2}$  is the spectral density of the amplifier voltage noise ( $0.5 \text{ nV}/\sqrt{\text{Hz}}$  at 10 Hz). The SQUID sensors have been characterized at liquid helium temperature, exhibiting a critical current of  $33 \mu\text{A}$ .

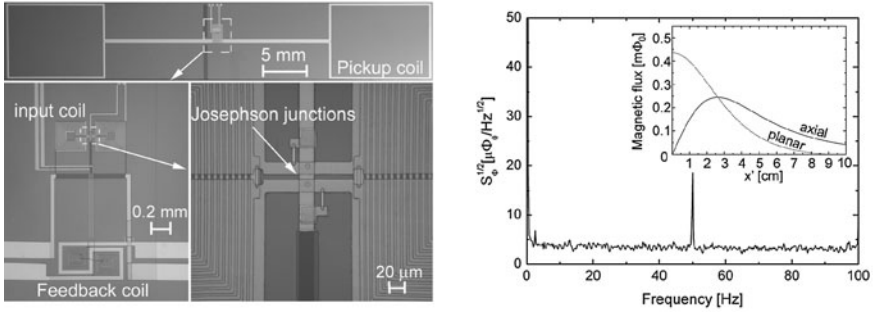


**Fig. 45.2** Picture of a fully integrated planar gradiometer showing the particulars of feedback and input coils and of the Josephson junctions (*left figure*). In the right figure the magnetic flux noise spectral density measured at  $T = 4.2$  K in FLL configuration is shown. The inset shows the net magnetic fluxes of the gradiometers in both planar and axial configuration as function of the off-axis dipole position  $x'$

A maximum  $V_\phi$  value of  $500 \mu\text{V}/\Phi_0$  can be evaluated from the  $V-\Phi$  characteristics that has a voltage swing of  $65 \mu\text{V}$ . The magnetic field sensitivity  $B_\phi$  referred to the single pick-up coil is about  $1 \text{ nT}/\Phi_0$ . The magnetic flux noise spectral density of the sensor, measured in flux looked loop without any high magnetic permeability shields was  $3 \mu\Phi_0/\sqrt{\text{Hz}}$ , corresponding to a magnetic field noise referred to the single pick-up coil of  $3 \text{ fT}/\sqrt{\text{Hz}}$ . Being a baseline length  $d = 50 \text{ mm}$ , the resulting spectral density of the field gradient noise is  $0.6 \text{ fT}/(\text{cm} \cdot \sqrt{\text{Hz}})$  [9].

In order to verify the device effectiveness for biomagnetic imaging, the magnetic responses of this planar sensor, in a vertical arrangement, to a current dipole has been computed. The results has been compared with those relative to a first order axial gradiometer having the same baseline, pick-up coil's size, and the same SQUID design parameters.

Following the same procedure reported in Ref. [6], the net device flux, for planar and axial configuration, is obtained by taking the difference of the magnetic fluxes treading the bottom coil and the top one ( $\Phi_N^P = \Phi_B^P - \Phi_T^P$ ). The output magnetic flux of the sensors, given by  $\Phi_S = G_\Phi \cdot \Phi_N^P$ , where  $G_\Phi = M_i / (L_p + L_i)$  is the flux gain [6], are reported in Fig. 45.2.

For a small range of off-axis distance  $x'$  around the peaks, the magnetic strengths of the planar gradiometer are appreciably greater than the axial ones; For longer  $x'$  distance, the magnetic strengths of the planar device falls faster than the axial one; however, in multichannel systems, the dipole sources having a  $x'$  distance greater than 2–4 cm can be effectively investigated by the neighboring sensors. The curves have been computed using for both sensors a current dipole strength ( $p_y = 10 \text{ nA}\cdot\text{m}$ ), a flux gain  $G_\Phi = 0.02$  and a distance between the current dipole and sensor of 4 cm [9].

### 45.3 Conclusions

A miniaturized dc SQUID magnetometer and a long baseline planar SQUID gradiometer, based on niobium technology, have been presented. The effectiveness of these device designs has been confirmed by both the experimental results and numerical simulations of the output magnetic flux. On the basis of such results, the sensors are suitable for high sensitivity applications such as the systems for biomagnetic imaging

Moreover, the miniaturized magnetometer is very useful when a large sensor density is required while the planar gradiometer can be employed in multichannel system working in a soft shielded environment.

### References

1. Clarke J, Braginski AI (2004) Applications of SQUID and SQUID system. In: Clarke J, Braginski, AI (eds), Weinheim The SQUID Handbook, vol 2. Wiley, New York
2. Enpuku K, Muta T, Yoshida K, Ire F (1985). Noise characteristics of a dc SQUID with a resistively shunted inductance. *J Appl Phys* 58:1916
3. Drung D (1996). Advanced SQUID read-out electronics. In: Weinstock H (ed) SQUID sensors: fundamentals, fabrication and application, series E, vol. 329, Kluwer Academic, Dordrecht, p 63
4. Granata C, Vettoliere A, Russo M (2006). Improved superconducting quantum interference device magnetometer for low cross talk operation. *Appl Phys Lett* 88:212506
5. Granata C, Vettoliere A, Russo M (2007) Miniaturized superconducting quantum interference magnetometers for high sensitivity applications. *Appl Phys Lett* 91:122509
6. Granata C, Vettoliere A, Rombetto S, Nappi C, Russo M (2008) Performance of compact integrated magnetometer for biomagnetic imaging. *J Appl Phys* 104:073905
7. Vrba J, Robinson SE (2002). SQUID sensor array configurations for magnetoencephalography applications. *Supercond Sci Technol* 15:R51
8. Stolz R, Fritzsche L, Meyer H-G (1999). LTS SQUID sensor with a new configuration. *Supercond Sci Technol* 12:806
9. Granata C, Vettoliere A, Lisitskiy M, Nappi C, Russo M (2009) Long baseline planar superconducting gradiometer for biomagnetic imaging. *Appl Phys Lett* 95:042502